

# Mimicking nitrogenase

Ian Dance

Received 28th October 2009, Accepted 17th December 2009

First published as an Advance Article on the web 28th January 2010

DOI: 10.1039/b922606k

In seeking to mimic the hydrogenation of  $N_2$  to  $NH_3$  as effected under mild conditions by the enzyme nitrogenase, three classes of known metal sulfide clusters that resemble the  $NFe_7MoS_9$  core of FeMo-co, the active site of nitrogenase, have been assessed theoretically. The assessment has been made in the context of the previously proposed mechanism for nitrogenase, in which protons are relayed to FeMo-co, where, as hydrogen atoms accumulated on Fe and S atoms, they transfer to bound  $N_2$  and subsequent intermediates in a critical sequence of intramolecular hydrogenations, probably accelerated by H atom tunneling. The three model systems possess the  $X^cFe_4S_4$  face which is the key active site of FeMo-co (X is most probably N in FeMo-co, and is S in the models). The most promising functional models are based on clusters **MI**,  $\{(tpb)Mo(\mu_3-S)_3Fe_2(Fe-L)S^c(\mu-S)_2(Fe-L)Fe_2(\mu_3-S)_3Mo(tpb)\}$  [tpb = tris(1-pyrazolyl)hydroborate], for which syntheses are well developed. The assessment is based on the ability of the models to mimic the intermediates in the FeMo-co mechanism, as determined by density functional simulations. The elaborations of **MI** required to mimic the FeMo-co behaviour are described. These include modification of the tpb ligands to control the coordination at the Fe atoms, to provide for the proton relay functionality, and to prevent unwanted reactivity at other Fe and S atoms. Literature references with prescriptions for synthesis of the predicted homogeneous catalysts are provided. Further, in view of the similarities between the model systems and the P-cluster of nitrogenase, it is speculated that the P-cluster could be a relic catalytic site for  $N_2$  reduction.

## Introduction

This paper is about the fixation of dinitrogen to ammonia, an inherently difficult reaction. The biological process, a crucial component of the biospheric nitrogen cycle and essential to all life on earth, is effected under mild conditions by nitrogenase enzymes in bacteria.<sup>1-5</sup> The industrial process, refined from the pioneering work of Haber and Bosch,<sup>6</sup> is an entirely different process for the synthesis of ammonia using heterogeneous catalysis at high temperature and pressure, through a mechanism involving

the combination of surface bound N atoms and H atoms.<sup>7</sup> The essentiality of metal sites in the biological and industrial processes has stimulated much research on the coordination chemistry of  $N_2$ ,<sup>8-12</sup> and therefrom to its activation and reduction under homogeneous conditions.<sup>13-17</sup> One of these systems, a mono-molybdenum complex with strong steric hindrance, leads to catalytic amounts of ammonia with limited turnover, but the mixture has to be manipulated to minimise short-circuiting formation of  $H_2$  by the reductant and proton source.<sup>18,19</sup> Some very interesting and promising interconversions of mono-Fe complexes containing  $N_2$ ,  $N_2H_2$ ,  $N_2H_4$ ,  $H_2$  and H have been described recently.<sup>20-26</sup>

Can the chemistry of the enzymatic process be used to design and create synthetic homogeneous catalysts for the reduction of  $N_2$  to  $NH_3$ ?

While the biochemical aspects of nitrogenase are relatively well understood,<sup>5,27-32</sup> the chemical mechanism is experimentally elusive.<sup>33</sup> The structures of the two proteins involved, an Fe protein and a MoFe protein, are known, as is the process in which they dock to initiate the hydrolysis of ATP and the transfer of an electron first to a redox-active P-cluster in the MoFe protein, and thence to the catalytic site, the Fe–Mo cofactor, or FeMo-co. A key part of the mechanism of nitrogenase is the involvement of  $H_2$  as both product and inhibitor:<sup>34</sup> the stoichiometry of the nitrogenase catalysis is close to  $N_2 + 8e^- + 8H^+ \rightarrow 2NH_3 + H_2$ . The abiological reaction  $D_2 + 2e^- + 2H^+ \rightarrow 2HD$ , which is  $N_2$  dependent and kinetically related to  $N_2$  reduction, provides key data for the testing of mechanisms.<sup>35,36</sup> Much kinetic and spectroscopic data have provided a good picture of the sequence of biochemical events through the multiple cycles involving electrons,  $N_2$ ,  $H_2$ ,  $D_2$  and  $NH_3$ .<sup>29,37</sup>

School of Chemistry, University of New South Wales, Sydney, 2052, Australia. E-mail: i.dance@unsw.edu.au



Ian Dance

*Ian Dance is Emeritus Professor of Chemistry at the University of New South Wales and a Fellow of the Australian Academy of Science. He has directed research programs on the synthesis and characterisation of polymetallic metal thiolates, metal chalcogenide clusters, solid state inclusion phenomena, supramolecular inorganic chemistry and crystal packing analysis, gas phase inorganic chemistry, metallocarbohedrenes and metal-carbon clusters,*

*applications of density functional theory, and the chemical mechanism of the biological fixation of nitrogen.*

The structure of FeMo-co<sup>38</sup> is shown in Fig. 1. The cluster core has the composition N<sup>c</sup>Fe<sub>7</sub>MoS<sub>9</sub> (the elemental identity of the central atom is not yet proven experimentally, but N is more likely than the alternatives C or O<sup>39-43</sup>), with Fe at one end coordinated to a cysteine while the Mo is additionally coordinated by histidine and homocitrate.

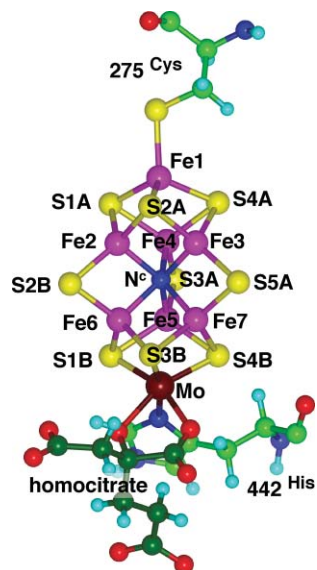


**Fig. 1** The resting structure of protein-bound FeMo-co: atom and residue labeling are from PDB 1M1N.

The behaviours of modified enzymes with mutated residues surrounding FeMo-co have indicated clearly that the catalytic site is the vicinity of Fe6 and Fe2 (Fig. 1).<sup>5,44,45</sup> In conjunction with this, careful and ingenious experimentation at low temperatures with wild type and mutant enzymes has enabled the trapping of species apparently containing bound H, N<sub>2</sub>, N<sub>2</sub>H<sub>2</sub> and N<sub>2</sub>H<sub>4</sub>, although structural characterisation of these is still in early stages.<sup>5,46-51</sup> Alkynes are alternative substrates for nitrogenase, and most success has come in characterising intermediates in alkyne reactions. The fact that the enzyme is almost spectroscopically quiet during turnover, as well as the fact that unavoidable protons compete as oxidising reactant, frustrate experimental investigation of the chemical mechanism. A synthetic cluster with the structure of FeMo-co is not yet available.<sup>52-54</sup>

In summary, the structure of the catalytically active site (in its resting state) is known, and valiant experimental work on the reactivity has yielded some interesting but mechanistically inconclusive information. In particular, there is no atomic level information about the most energetically difficult first stage in reducing N<sub>2</sub>. The stage for the molecular dance that is biological nitrogen fixation is clearly set, the dancers are known, the rhythm is evident, and some scenes have been glimpsed, but the choreography is elusive.

## Theoretical approach to mechanism

With scarce experimental information about the mechanism of catalysis at FeMo-co, powerful theoretical simulation techniques are valuable and can be used to expand the experimental information.<sup>40,41,55-64</sup> I have applied density functional calculations

to investigation of the coordination chemistry of FeMo-co. This has yielded much information in three areas.<sup>65</sup> (a) One is the general behaviour of FeMo-co as a multimetal site for the binding of ligands, and has revealed that the pertinent Fe atoms can bind one or two ligands with various Fe coordination stereochemistries, and that the central atom N<sup>c</sup> is the mediator for coordinative allostereism involving Fe2 and Fe6. The well-defined *endo*- and *exo*- Fe coordination positions are illustrated in Fig. 2 for Fe6. (b) The second collection of information involves the binding of N<sub>2</sub>, H and H<sub>2</sub> to FeMo-co,<sup>66,67</sup> including the binding of multiple H atoms (at S/Fe) and combinations of N<sub>2</sub>, H and/or H<sub>2</sub>. This work included calculation of energy profiles for the association-dissociation of these ligands, and their dependence on the coordination status of FeMo-co. (c) The third outcome from this work was recognition that the μ<sub>3</sub>-S atom labelled S3B (Fig. 1) could be the site of protonation of FeMo-co (from a conserved proton relay chain through the MoFe protein).<sup>66</sup> This, with the variability of both configuration and conformation of the resulting S3B-H, allows sequential relay of multiple H atoms to FeMo-co. This is significant, because the protein surrounding the catalytically active face of FeMo-co is largely anhydrous and hydrophobic, and there is no evident mechanism for the provision of the six or more protons required for one catalytic cycle.

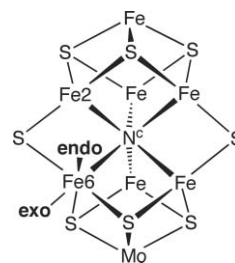


**Fig. 2** The *exo* and *endo* coordination positions (*trans* and *cis* to N<sup>c</sup> respectively) for Fe6: analogous positions occur at Fe2.

This research introduces a new mechanistic paradigm for catalyses effected by nitrogenase, which is that the reductions occur by intramolecular transfer of H atoms to bound substrates and intermediates. The traditional concept was that FeMo-co acquires electrons, a number of which are required before it is able to bind N<sub>2</sub> or other substrates, and then that protons are provided from surrounding protein residues (and/or water) to the electron-rich bound substrates. I believe that all of the reductive steps occur instead through short-distance intramolecular H atom transfer, fully controlled by the atoms of FeMo-co. The well-defined proton relay to S3B, triggered by electronation of FeMo-co, generates the H atoms on S3B, which are subsequently transferred to other atoms of FeMo-co and to bound substrate and intermediates.<sup>66</sup> It is postulated that there is a single path for replenishable serial supply of protons which become H atoms on FeMo-co, migrating to become S-H and Fe-H donors to N<sub>2</sub> and to the intermediates that follow. This paradigm of controlled intramolecular hydrogenation (as opposed to exogenous protonation), and its elaboration involving the importance of the sequences of hydrogen transfer events,<sup>65</sup> allows explanations for a number of observations of the reactivity of nitrogenase with C<sub>2</sub>H<sub>2</sub> and N<sub>2</sub>.<sup>68</sup>

This combined knowledge of the coordination chemistry of FeMo-co, and of the relevant principles (largely unprecedented),

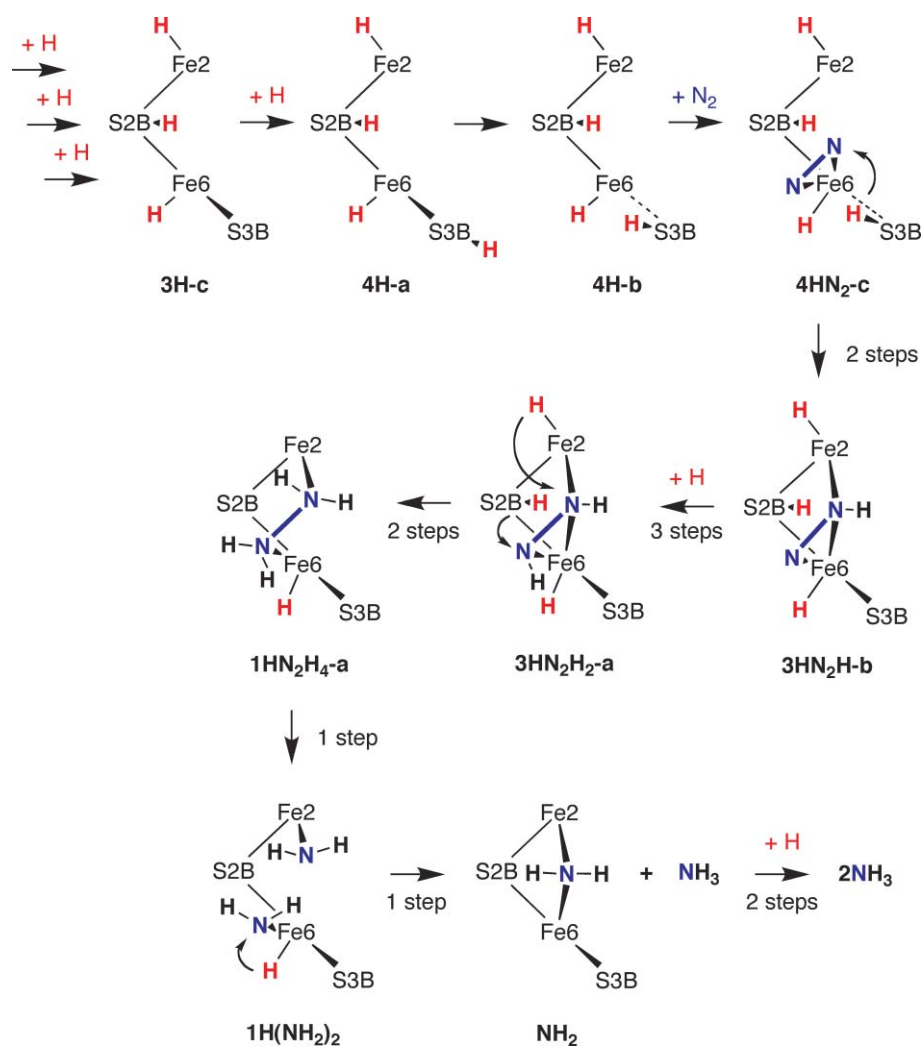


**Fig. 3** An abbreviated presentation of the previously described mechanism for hydrogenation of  $N_2$  to  $NH_3$ ,<sup>69</sup> showing key intermediates. The atoms Fe2, S2B, Fe6 and S3B only of FeMo-co are depicted: H atoms on FeMo-co are red, while those transferred to  $N_2$  are black. Each of the six +H additions involves prior electronation of FeMo-co and proton relay to S3B.

together with the concept of intramolecular hydrogenation as the fundamental process, allowed further investigation of the probable mechanism by which FeMo-co converts  $N_2$  to  $NH_3$ . The multiple possibilities for the sequences of bond breaking and making steps were simulated and assessed *via* their activation energies, leading to a proposed mechanism for the catalysis.<sup>69</sup> The full mechanism has 21 steps. Fig. 3 provides an abbreviated view of some significant intermediates, labeled as previously.<sup>69</sup> Fig. 4 shows some optimised structures, demonstrating the different coordination geometries for Fe and the elongations of  $N^c$ -Fe (eg **3H-c**, **4H-a**, **4H-b**, **4HN<sub>2</sub>-c**, **3HN<sub>2</sub>H-b**, **1HN<sub>2</sub>H<sub>4</sub>-a**) and Fe-S interactions (eg **4H-a**, **4H-b**, **4HN<sub>2</sub>-c**), as well as the variability of configurations/conformations at S3B when hydrogenated (eg **4H-a**, **4H-b**). **4HN<sub>2</sub>-c** is the key intermediate leading to the first transfer of H from S3B to  $\eta^2$ -bound  $N_2$ : the similarity between structures **4HN<sub>2</sub>-c** and **3HN<sub>2</sub>H-b** and the relatively short distance for H to traverse is evident in Fig. 4. Because **3HN<sub>2</sub>H-b** has  $N_2H$  locked into a bridging position between Fe2 and Fe6, similar short H-transfer distances occur when subsequent H atoms transfer from

S3B, Fe2, S2B and Fe6. The trajectories for these intramolecular H-transfer steps are very similar to those for other enzymes where H atom tunneling is established, and I have proposed that part of the catalytic rate acceleration of FeMo-co is due to comparable H atom tunneling.<sup>70</sup>

This summary of the proposed enzymatic mechanism for reduction of  $N_2$  leads to specification of the attributes required of a synthetic mimicking catalyst.

### Attributes of a mimicking catalyst

The attributes required for a catalyst system mimicking FeMo-co in nitrogenase are considered in two parts, first for the cluster core which effects the intramolecular H atom transfer steps, and then for the ligand surrounds which must control the proton transfer to the cluster and inhibit alternative interfering reactions.

The minimal components of a cluster able to mimic the behaviour of FeMo-co are proposed to be those of structure **1**. The rationale for these components is:

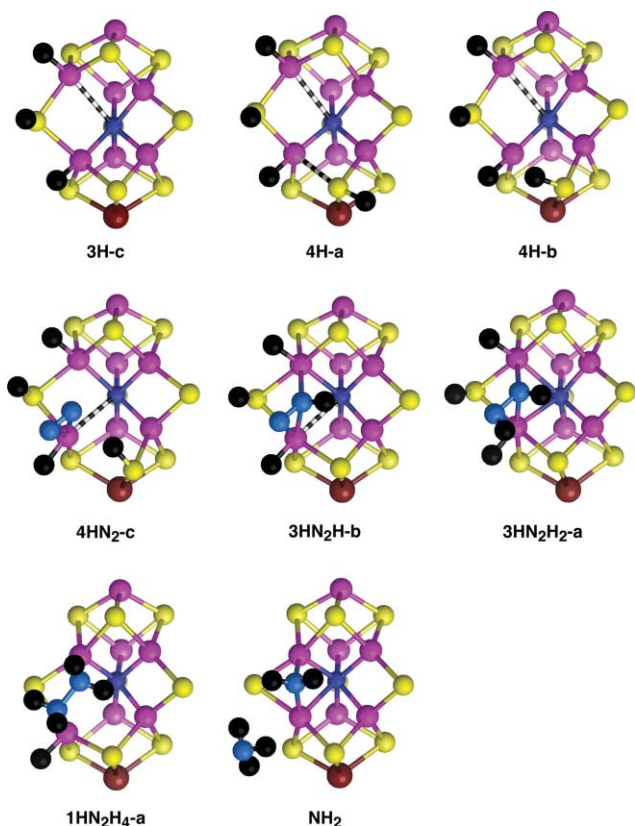
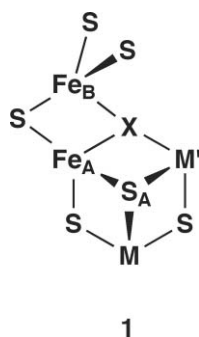


**Fig. 4** Optimised structures of some key intermediates in the proposed mechanism (cf Fig. 3). The view direction is perpendicular to the Fe<sub>2</sub>,Fe<sub>3</sub>,Fe<sub>6</sub>,Fe<sub>7</sub> face (similar to Fig. 1). Fe magenta, S yellow, Mo brown, N blue, H black: the terminal ligands bound to Fe<sub>1</sub> and Mo are not shown. N<sup>c</sup>-Fe and Fe-S distances in the range 2.5-3 Å are marked as black and white broken bonds.



1. Two adjacent Fe atoms (Fe<sub>A</sub>, Fe<sub>B</sub>) are to be bridged by μ<sub>3</sub>-S [Fe<sub>A</sub> ≡ Fe<sub>6</sub>, Fe<sub>B</sub> ≡ Fe<sub>2</sub> (Fig. 1)].

2. A monatomic ligand (X) also bridges the two Fe atoms, and is further coordinated by other M' atoms in the cluster. X must be able to sustain variable coordination, through variation of the X-Fe and X-M' distances. This variation of Fe-X coordination correlates with additional coordination of Fe by substrates N<sub>2</sub> and intermediates N<sub>2</sub>H<sub>x</sub>, NH<sub>x</sub>. X should be able to exert and control coordinative allostereism at Fe<sub>A</sub> and Fe<sub>B</sub>.

3. There should be two additional coordination sites at each of Fe<sub>A</sub> and Fe<sub>B</sub> [analogous to the *endo*, *exo* sites of FeMo-co (Fig. 2)].

4. One of the Fe atoms (Fe<sub>A</sub>) is to be the initial N<sub>2</sub> binding site.

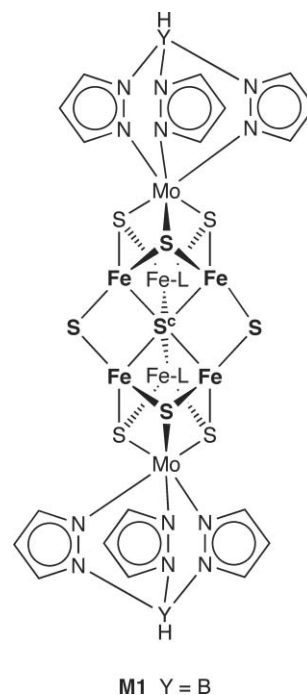
5. The Fe and S atoms are able to bear H atoms.

6. S<sub>A</sub>, a μ<sub>3</sub>-S ligand on Fe<sub>A</sub>, is able to be protonated, and, through variation of its Fe/M-S bond lengths and Fe/M-S-H stereochemistry, is able to transfer H atoms to Fe<sub>A</sub> and to substrates and intermediates bound to Fe<sub>A</sub> [S<sub>A</sub> ≡ S3B (Fig. 1)].

Clearly the cluster must contain additional atoms, completing the coordination of M, X, M' and the upper S atoms bound to Fe<sub>B</sub>.

## Existing suitable systems

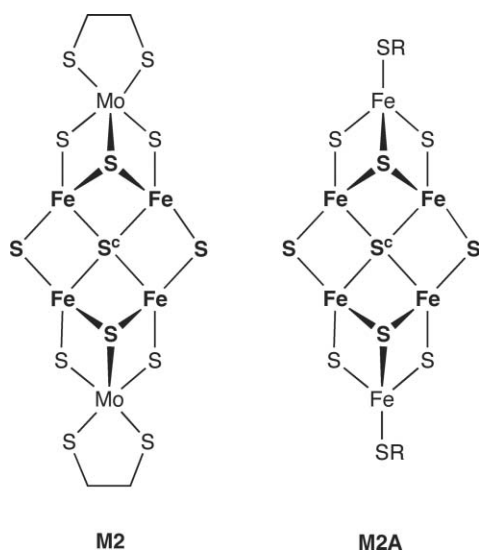
Three well-known cluster systems possess these attributes and resemble the FeMo-co site. One is **M1**, investigated in detail by Holm *et al.* with tris(1-pyrazolyl)borate (Y = B) providing terminal coordination of Mo. Six Fe atoms from two cubanoid MoFe<sub>3</sub>S<sub>3</sub> moieties surround a central μ<sub>6</sub>-S atom, in distorted trigonal prismatic geometry; two of the Fe-Fe edges of the trigonal prism are bridged by μ-S atoms, while the remaining two Fe atoms each support a terminal ligand (L) instead. While the investigators of this system have drawn attention to its metrical similarities with the reduced state (P<sup>N</sup>) of the P-cluster of nitrogenase,<sup>71</sup> **M1** also has close chemical similarities with FeMo-co, and in particular the pertinent Fe<sub>4</sub>(μ-S)<sub>2</sub>(μ<sub>3</sub>-S)<sub>2</sub> face over a μ<sub>6</sub> bridging atom is present (hereafter the central μ<sub>6</sub>-S atom is labelled S<sup>c</sup>, analogous to N<sup>c</sup> of FeMo-co)



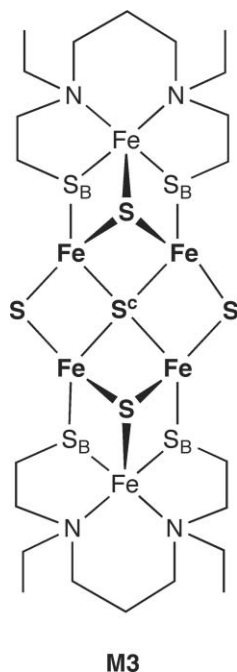
Well characterised **M1**(L)<sub>2</sub> derivatives are [M1(SH)<sub>2</sub>]<sup>3-</sup>,<sup>72</sup> [M1(SPh)<sub>2</sub>]<sup>3-</sup>,<sup>71</sup> [M1(CN)<sub>2</sub>]<sup>3-</sup>,<sup>73</sup> [M1(F)<sub>2</sub>]<sup>3-</sup>,<sup>74</sup> [M1(OH)<sub>2</sub>]<sup>3-</sup>,<sup>75</sup> [M1(OMe)<sub>2</sub>]<sup>3-</sup>,<sup>75</sup> [M1(OH)(OC(Me)NH)]<sup>3-</sup>.<sup>75</sup> The vanadium analog, [M1(V)(SH)<sub>2</sub>]<sup>4+</sup>, is known.<sup>76</sup> The preparative pathways to **M1** derivatives are well understood.<sup>71-73</sup> [M1(SH)<sub>2</sub>]<sup>3-</sup> is in a moderately reduced state, as indicated by 2-/3- oxidation at -1.09v (*vs* SCE), further 2-/1- oxidation at -0.45v, and 3-/4- reduction at -1.80v.<sup>73</sup>

The second potential model is **M2**,<sup>77</sup> which is related to a collection of molecules **M2A** first reported more than 25 years ago.<sup>78-80</sup> These molecules possess the requisite Fe<sub>4</sub>(μ<sub>3</sub>-S)<sub>2</sub>(μ-S)<sub>2</sub> face, with a centering S<sup>c</sup> atom that is four coordinate. For reasons that will become apparent I will focus on **M2** rather than **M2A**. The

preparations of  $(\text{Bu}_4\text{N})_4[\text{M2}]^{4-}$  and of its one-electron oxidised form  $(\text{Bu}_4\text{N})_3[\text{M2}]^{3-}$  are established.<sup>77</sup>



The third potential model system is **M3**.<sup>81</sup> This retains the same central  $\text{S}^c\text{Fe}_4(\mu_3\text{-S})_2(\mu\text{-S})_2$  face as the previous models, but the flanking sulfur ligands  $\text{S}_B$  that link this face to the end sections are thiolate rather than sulfide. These  $\text{S}_B$  ligands are not involved in the putative mechanism of FeMo-co, but rather have a structural role, and there is no *a priori* reason to expect that thiolate in these positions would be disadvantageous. The preparation of **M3** involves three high-yield steps, and permits opportunities for modification of the 3,7-diazanonane-1,9-dithiol ligand to elaborate the model. Uncharged **M3** undergoes electrochemical reductions at -0.83 and -1.63v (*vs* SCE).



An immediate question about these models is their geometrical similarity to FeMo-co. Clearly  $\text{S}^c$  is larger than  $\text{N}^c$ . One consequence of this is that  $\text{S}^c$  at the rear folds the  $\text{Fe}_4\text{S}_4$  face forwards about the  $(\mu\text{-S}) \cdots (\mu\text{-S})$  vector, causing the  $(\mu_3\text{-S}) \cdots (\mu_3\text{-S})$  distance

**Table 1** Comparative distances (Å) for the significant front face of FeMo-co, **M1**, **M2** and **M3**

	FeMo-co [PDB 1M1N]	$[\text{M1}(\text{F})_2]^{3-}$ [CSD VEGCAM]	<b>M2</b> [CSD FATWIG01]	<b>M3</b> [CSD HILWAA]
$\mu_3\text{-S} \cdots \mu_3\text{-S}$	5.00	4.16	4.38	4.66
$\mu\text{-S} \cdots \mu\text{-S}$	5.70	5.95	5.85	5.77
$\text{Fe} \cdots \text{Fe}$ axial, transverse	2.58, 2.65	2.79, 2.68	2.75, 2.66	2.72, 2.66
$\text{X}^c\text{-Fe}$	1.99–2.09	2.41	2.33	2.30–2.32

to shorten. This effect is most pronounced in **M1**, as illustrated in Fig. 5. Table 1 compares the front-face geometries for FeMo-co and the three models. The least distortion away from the FeMo-co geometry occurs in **M3**, which, apart from the inevitable expansion of the  $\text{X}^c\text{-Fe}$  distances by 0.3 Å, is remarkably similar to FeMo-co. However, the flexibility of the model is even more important, and the loose connectivity of **M2** indicates non-rigidity. These considerations are addressed in the results below.

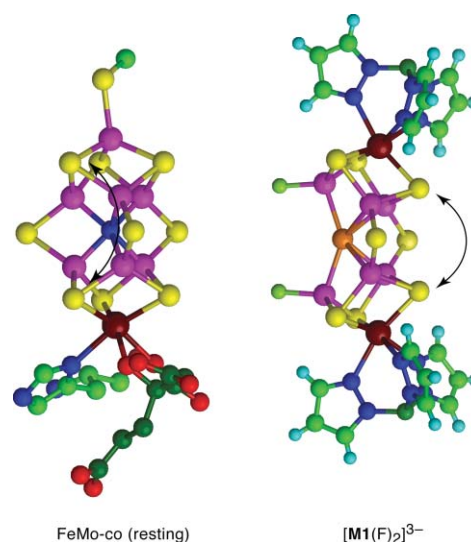


**Fig. 5** Comparative side views of FeMo-co (structure PDB 1M1N) and  $[\text{M1}(\text{F})_2]^{3-}$  (structure CSD VEGCAM,  $\text{S}^c$  orange) to show the relative opening of the rear  $\text{HS-Fe}(\mu_6\text{-S})\text{-Fe-SH}$  section and concomitant closing of  $(\mu_3\text{-S}) \cdots (\mu_3\text{-S})$  (arrowed) on the front  $\text{Fe}_4\text{S}_4$  face.

### Theoretical simulations of the catalytic abilities of the models

In order to test the suitabilities of these clusters as systems to mimic the catalytic steps of FeMo-co, I have undertaken density functional calculations of some species analogous to intermediates in the proposed mechanism (Fig. 3, 4). These are exploratory calculations, directed towards the first objective of this research which is to determine whether **M1**, **M2** or **M3** are worth pursuing as mimics. This is done by calculating and examining the geometries of the intermediates that the mimics would pass through during the catalysis, in order to eliminate unlikely prospects. The next stage of the research, in conjunction with syntheses of models possessing suitably elaborated ligands (see below), involves more detailed computational simulation of

the steps in the mechanism by calculation of transition states and reaction profiles.

The computational procedures employed in the present work are the same as those used in previous work on FeMo-co: details and validations have been described.<sup>66,67,69</sup>

It is important to recognise that these models, like FeMo-co, have variable molecular oxidation states (expressed as overall charges), each of which has a number of electronic states close in energy to the ground state. Full calculation of the structures of intermediates and transition states in a mechanism for the reactions of FeMo-co or of these comparable models involves consideration of these variables, which is a moderately laborious although straightforward task. The different electronic states of clusters such as these are specified and controlled in terms of the spin densities on the individual metal atoms.<sup>65,82,83</sup> The spin and electronic states of intermediates in the mechanism were fully investigated in the previous work on FeMo-co,<sup>69</sup> but limited exploration of alternative electronic states is implicit in the following results on models. The cluster systems **M2** and **M2A** were included in a previous correlation of HOMO energy with cluster redox potential.<sup>43</sup>

As described in the previous section, **M1** is folded in a way that constricts the reaction face. Initial calculations with **M1** showed that it has difficulties binding  $\eta^2$ -N<sub>2</sub> and therefore several modifications of **M1** were investigated. These are described below, after results for **M2** and **M3**.

Fig. 6 depicts optimised structures for **M2** and **M3** composed as some of the FeMo-co mechanism intermediates: species labels have the FeMo-co intermediate name appended, after/. Several general results are evident. (a) Loading the models with H atoms on the appropriate S and Fe atoms is feasible. (b) The **M2** structures are less rigid than **M3** structures. (c) The S<sup>c</sup> atom can vary its coordination by elongation of S<sup>c</sup>-Fe, and if this occurs it usually involves one S<sup>c</sup>-Fe interaction (only one structure, **M2/3H-c**, has two long S<sup>c</sup>-Fe interactions). (d) Intermediates at the N<sub>2</sub>H, N<sub>2</sub>H<sub>2</sub>, N<sub>2</sub>H<sub>4</sub> stages of the mechanism, such as **3HN<sub>2</sub>H-b**, **3HN<sub>2</sub>H<sub>2</sub>-a** and **1HN<sub>2</sub>H<sub>4</sub>-a**, are mimicked well by both **M2** and **M3**.

There is a specific issue with **M3**, where one of the thiolate ligand H atoms intrudes into the *exo*-Fe coordination domain, forcing an *exo*-Fe-H atom forwards such that the S<sup>c</sup>-Fe-H angles are reduced to ca 160°, and in **M3/4H-b** the *exo*-Fe6-H atom is close (1.9 Å) to S3B-H, and H<sub>2</sub> formation is a facile process. These H-H steric contacts are shown with black/blue stripes on structures in Fig. 6. One consequence of this ligand H atom is that an **M3** version of **4HN<sub>2</sub>-c**, requiring both *exo*-Fe6-H and *endo*-Fe6-( $\eta^2$ -N<sub>2</sub>), appears to be sterically impossible. Note that the comparable structures **M2/3HN<sub>2</sub>-a** and **M2/4HN<sub>2</sub>-c** are both feasible. Note also that **M3** with  $\eta^2$ -N<sub>2</sub> coordinated between the *exo* and *endo* positions of Fe6 is feasible, in structure **M3-( $\eta^2$ -N<sub>2</sub>)-Fe2H-S2BH** (Fig. 6).

Initial calculations of **M1** showed some difficulties with the binding of N<sub>2</sub> at the *endo* position of Fe6, possibly due to the crowding of the front face, and therefore modifications to obviate this were considered. The ligands L on the two rear Fe atoms of **M1** suggest the possibility of linkage by chelation or bridging, and in order to assess the effectiveness of this the modification **M1A** was evaluated: the two ligands, already known as monodentate thiolates, were replaced by bridging thiolate <sup>-</sup>SCH<sub>3</sub> (Fig. 7(b)). After optimisation of the core with this modification, the binding of N<sub>2</sub> was enabled. These calculations revealed another property of **M1** affecting its ability to mimic the functionality of

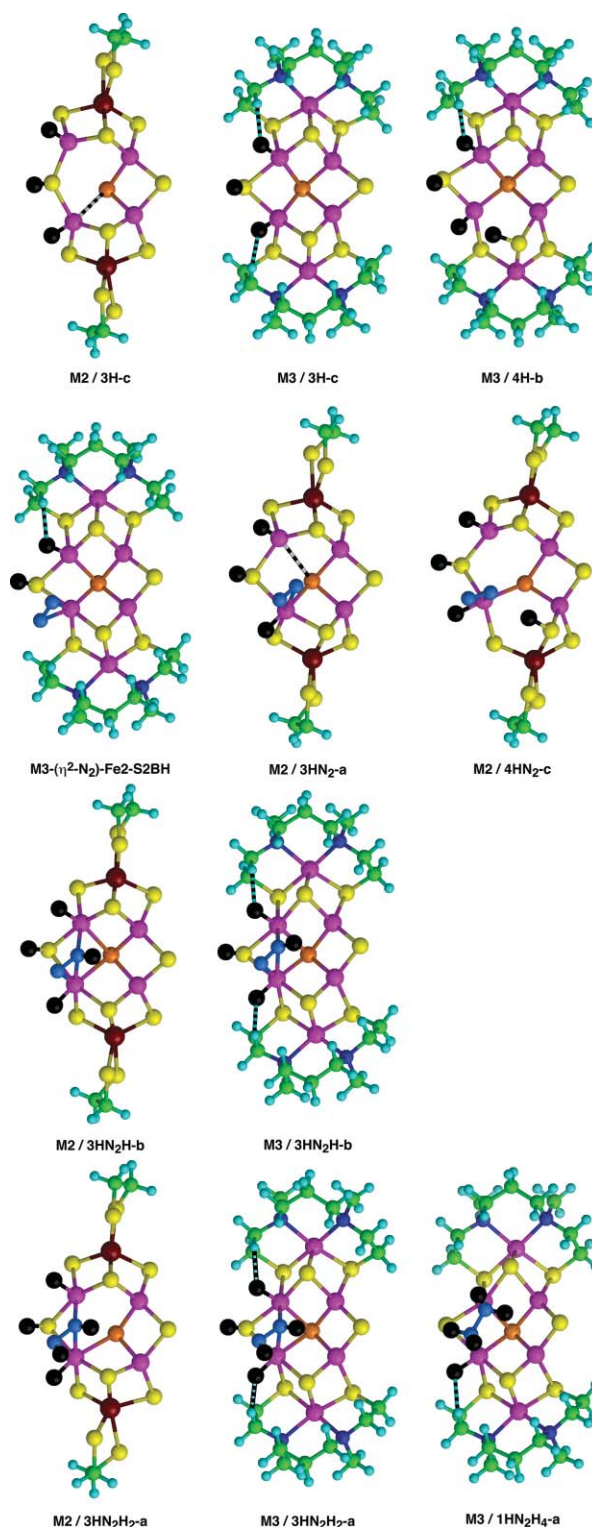


**Fig. 6** Optimised structures for **M2** and **M3** formulated as key intermediates in the FeMo-co mechanism, labeled as **model/intermediate**. Added H atoms are black; N<sub>2</sub> atoms are lighter blue; S<sup>c</sup> is orange; Fe-S interactions in the range 2.7 - 3.0 are marked as black and white broken bonds; black and blue striped contacts are close H-H interactions discussed in the text.

FeMo-co, which is that the 3-H atoms of the pyrazolyl groups of the tris(pyrazolyl) tripodal ligand hover over the *exo* coordination positions of the Fe atoms, and interfere with ligation in this

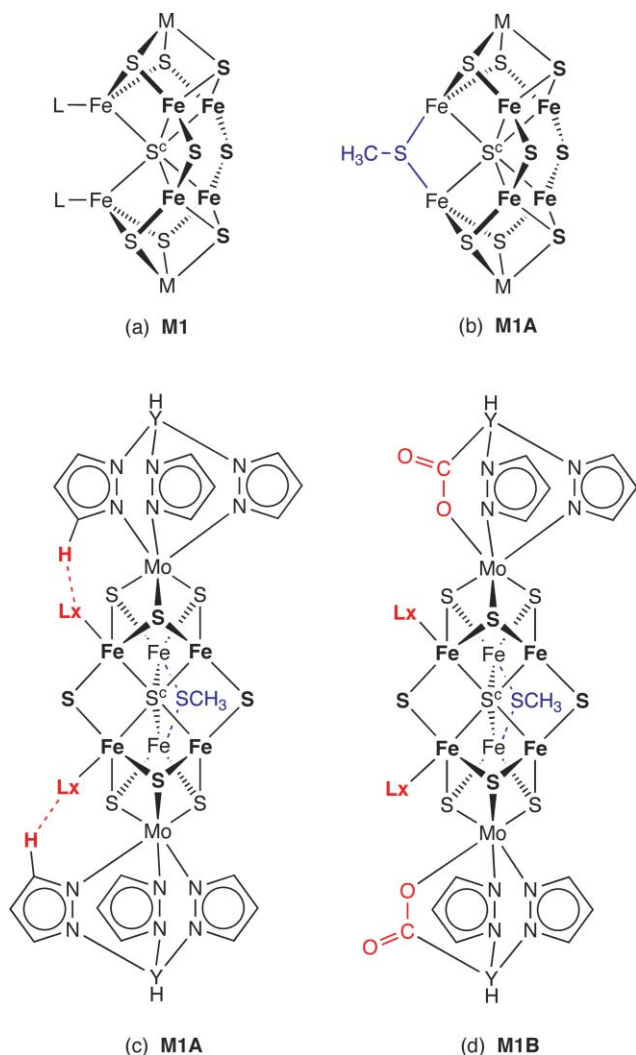


**Fig. 7** Modifications of **M1**. The rear thiolate bridge in place of the two monodentate ligands **L** is marked blue. (c) The interference between pyrazolyl **H** and ligands **Lx** in the *exo*-position of **Fe**. (d) Conversion of pyrazolyl to carboxylate in **M1B**.

position (Fig. 7(c)). *Exo*-coordination of **H** atoms at **Fe2** and **Fe6** is involved in the proposed mechanism for **FeMo-co**. Substitution of the pyrazolyl group with carboxylate, for example, removes this interference: model **M1B** has carboxylate substitutions close to both **Fe2** and **Fe6**, and therefore is able to accommodate *exo*-**Fe-Lx** ligands (Fig. 7(d)). Calculations also showed, as expected, negligible differences between complexes with tris(1-pyrazolyl)borate ( $Y = B$ ) or tris(1-pyrazolyl)methane ( $Y = C$ ) ligands.

Fig. 8 shows the optimised model **M1B** and how it would form some of the intermediates of the **FeMo-co** mechanism.

Structure **M1B**/( $NH_2$ )( $NH_3$ ) is different from structure  $NH_2$  in the **FeMo-co** mechanism (Fig. 4) in that the  $NH_3$  formed at the *exo*-**Fe6** position is still bound. In the **FeMo-co** mechanism this  $NH_3$  dissociates as it is formed. This difference could arise because the corresponding transition state for the severance of the **N-N** bond in the step  $1HN_2H_4-a \rightarrow 1H(NH_2)_2$  has not yet been determined for model **M1B**. Apart from this, all of the **M1B/intermediate** structures mimic the **FeMo-co** intermediates.

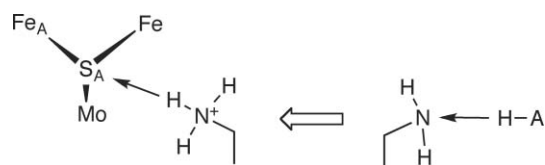
Details of the distances  $S^c-Fe$ ,  $(\mu_3-S) \cdots (\mu_3-S)$ , and  $Fe_A-S_A$  are contained in Table 2. Note that the  $S^c-Fe$  distances, which occur as  $6 \times 2.31 \text{ \AA}$  in **M1B**, can extend to  $2.53 \text{ \AA}$  for  $S^c-Fe_A$  and  $S^c-Fe_B$  in the intermediates (eg **M1B/3HN<sub>2</sub>H-b**), with concomitant shortening to  $2.20 \text{ \AA}$  of other  $S^c-Fe$ . This is analogous to the coordinative allostereism of  $N^c-Fe$  distances of **FeMo-co**,<sup>65</sup> but is smaller in magnitude. The important result is that the larger  $S^c$  atom is able to provide the appropriate **Fe** locations to support the various bindings of **H**,  $N_2$ ,  $N_2H_x$  and  $NH_x$  in the **M1B** intermediates. The similarity of **M1B/4HN<sub>2</sub>-c** (Fig. 8) and **FeMo-co/4HN<sub>2</sub>-c** (Fig. 4) is particularly significant, because this is the key intermediate preceding the first hydrogenation of  $N_2$ . The variability of the  $S_A-Fe_A$  distance, according to the hydrogenation of  $S_A$ , is comparable in the intermediates of **M1B** and **FeMo-co**, and is expected to yield similar reaction trajectories for **H**-transfer from  $S_A$ . It is concluded here that the cluster core of **M1B** is well-suited to mimic the catalytic steps proposed to occur in **FeMo-co**.

### Elaborations of the models: ligand requirements

In order to mimic the proposed nitrogenase mechanism, two additional features are required of the model system. One is a mediator for the serial supply of protons to  $S_A$ , where they become the **H** atoms to be used in the reduction. The second requirement is a peripheral ligand enclosure that blocks reactivity at **Fe** and **S** sites other than  $Fe_A$ ,  $Fe_B$  and  $S_A$  where the mechanism is controlled.

Considering first the elaborations of the ligands of **M1B** required to block unwanted reactivity, additional bulk can be introduced at the thiolate bridging the two rear **Fe** atoms, and at the 3 positions of the pyrazolyl rings (closest to the central cluster atoms). Model **M1B-a** has bridging *t*-butylthiolate (coloured blue), *i*-propyl substituents at the 3 positions of the two rear pyrazolyl ligands (red), and one 3-methylpyrazolyl ligand (green). Optimisation of this structure reveals that the two *i*-propyl substituents in the configuration shown effectively block access to  $Fe_E$ ,  $Fe_F$ , and the two  $\mu_3-S$  atoms bonded to each of these two **Fe** atoms, while the methyl substituent in the conformation shown blocks  $Fe_C$ . There are two possible configurations for the *i*-propyl substituents, and the alternative, with the two methyl groups directed towards the **Fe,S** atoms of the cluster, is too crowded, and on optimisation leads to partial dissociation of the pyrazolyl ligand: 3-(*t*-butyl) substitution of the pyrazolyl ligands would be inappropriate for the same reason.

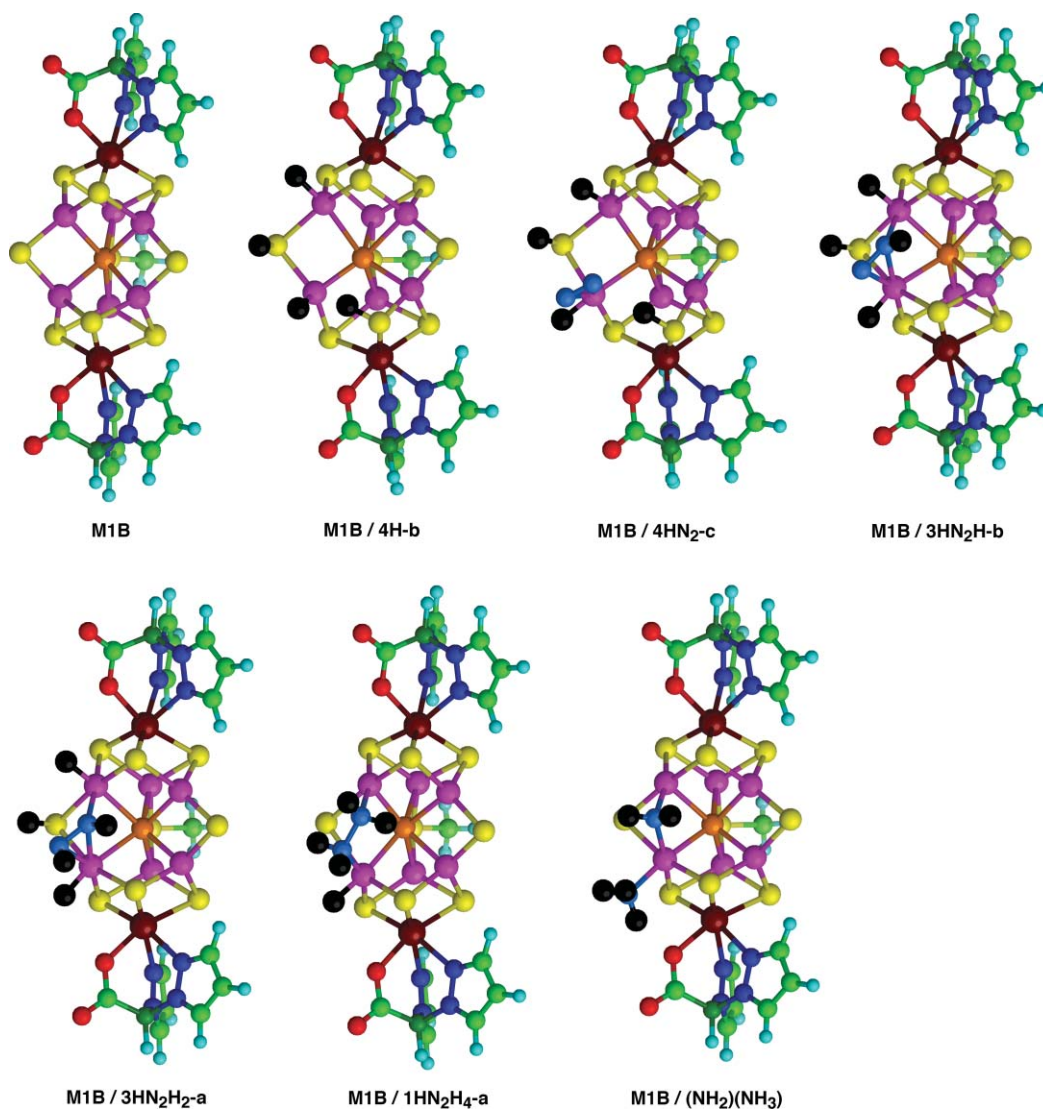
In nitrogenase it is proposed that there is relay of protons to  $S_A$  (ie **S3B**) through a conserved chain of water molecules held in place by surrounding protein. One key conserved water molecule has been identified as the terminus of the chain and the agent for protonation of  $S_A$ .<sup>66</sup> This protein-based structure is not easily mimicked, but an amine or alcohol function on a flexible arm attached to the ligand structure could relay protons from the exogenous acid **AH** to  $S_A$  (Scheme 1). An advantage of the **M1**



**Scheme 1**

**Table 2** Frontal ( $\mu_3\text{-S}$ )  $\cdots$  ( $\mu_3\text{-S}$ ) distances, Fe-S<sup>c</sup> distances, and Fe<sub>A</sub>-S<sub>A</sub> (Å) in **M1B/intermediate** structures

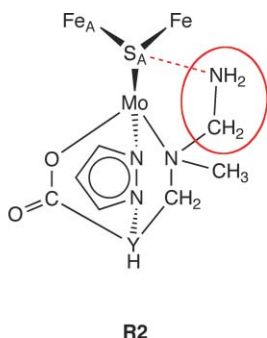
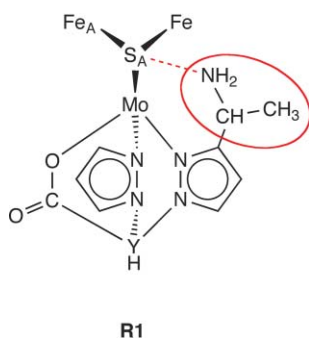
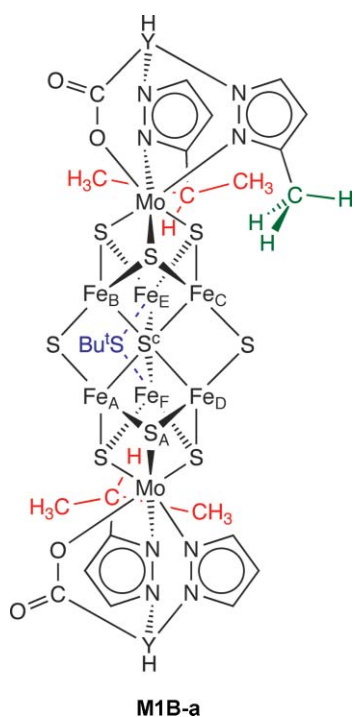
Intermediate	( $\mu_3\text{-S}$ ) $\cdots$ ( $\mu_3\text{-S}$ )	S <sup>c</sup> -Fe <sub>A</sub>	S <sup>c</sup> -Fe <sub>B</sub>	Other S <sup>c</sup> -Fe				Fe <sub>A</sub> -S <sub>A</sub>
<b>M1B</b>	4.86	2.32	2.31	2.30	2.32	2.30	2.29	2.28
<b>4H-b</b>	5.40	2.23	2.53	2.30	2.41	2.31	2.39	3.58
<b>4HN<sub>2</sub>-c</b>	5.67	2.44	2.39	2.34	2.29	2.32	2.35	3.83
<b>3HN<sub>2</sub>H-b</b>	4.78	2.49	2.52	2.22	2.33	2.20	2.32	2.42
<b>3HN<sub>2</sub>H<sub>2</sub>-a</b>	4.91	2.52	2.47	2.26	2.28	2.23	2.25	2.40
<b>1HN<sub>2</sub>H<sub>4</sub>-a</b>	5.35	2.45	2.23	2.35	2.32	2.38	2.41	2.32
<b>(NH<sub>2</sub>)(NH<sub>3</sub>)</b>	4.80	2.38	2.44	2.24	2.25	2.22	2.28	2.34

**Fig. 8** Optimised structures for **M1B** formulated as key intermediates in the FeMo-co mechanism, labeled as **M1B/intermediate**. Added H atoms are black; N<sub>2</sub> atoms are lighter blue; S<sup>c</sup> is orange.

model systems is that one of the pyrazolyl rings, that directed approximately towards Fe<sub>D</sub>, is on the side of S<sub>A</sub> opposite Fe<sub>A</sub>, and therefore is well placed to support the relay function.

Preliminary investigations have been made for two simple proton relay mimics, **R1** which has an amine function as part of the 3-substituent of the proximate pyrazolyl ligand, and **R2** in which the pyrazolyl ligand is replaced by a tertiary amine

ligating function, bearing a pendant primary amine as proton relay agent. **R1** and **R2** have differing conformational variability in the movement of the proton relay site to and from S<sub>A</sub>. Structure optimisations show that **R2** has some conformational difficulties, and would need redesign. However **R1** is able to form a hydrogen bond between the NH<sub>2</sub> donor and S<sub>A</sub> comparable with that of the enzyme. Calculations also show that addition of a proton to the



amine donor function leads to spontaneous transfer of the proton to  $S_A$ .

Fig. 9 shows front and back views of the optimised structure of **M1B-b**, which combines the ligand enclosure elements of **M1B-a** and the proton relay function of **R1**.

## Discussion

The three known Fe/S cluster systems, **M1**, **M2** and **M3**, and modifications mimic the active face of FeMo-co, and are able to sustain the intermediates of the proposed mechanism for the reaction  $N_2 + 6H^+ + 6e^- \rightarrow 2NH_3$  as catalysed at FeMo-co by nitrogenase. In the case of **M1** it is probable that the two rear Fe atoms should be tied together by a bridging or chelating ligand in order to closely mimic the FeMo-co behaviour. The central  $S^c$  atom of **M1**, **M2**, **M3** and modifications behaves similarly to the  $N^c$  atom of FeMo-co. Further, each of the mimics has a number of electronic and spin states (results not reported here), as does FeMo-co.

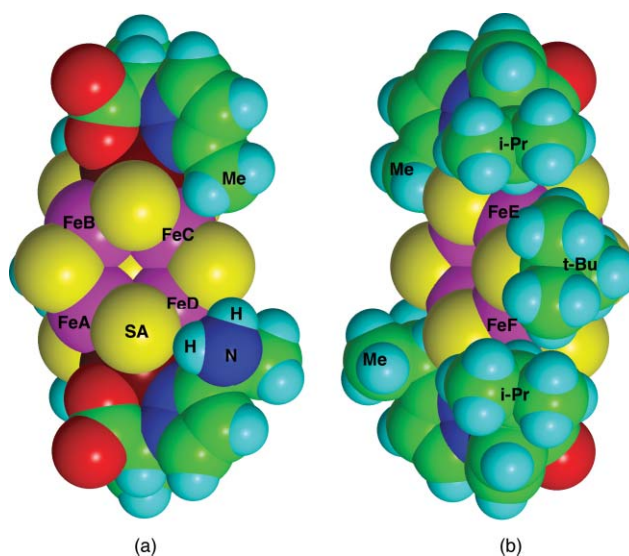
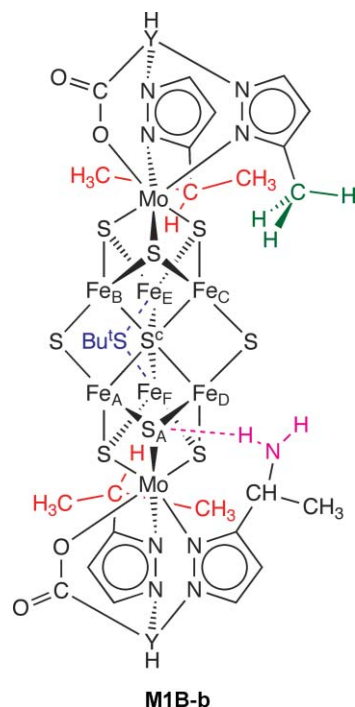
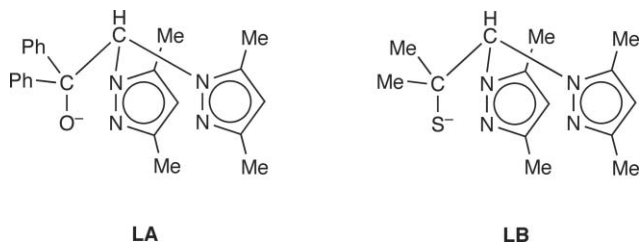


**Fig. 9** Front (a) and rear (b) views of the van der Waals surface of optimised model **M1B-b**, showing the relay  $HNH \cdots S_A$  hydrogen bond, and the blocking of Fe atoms and back S atoms by the alkyl substituents.

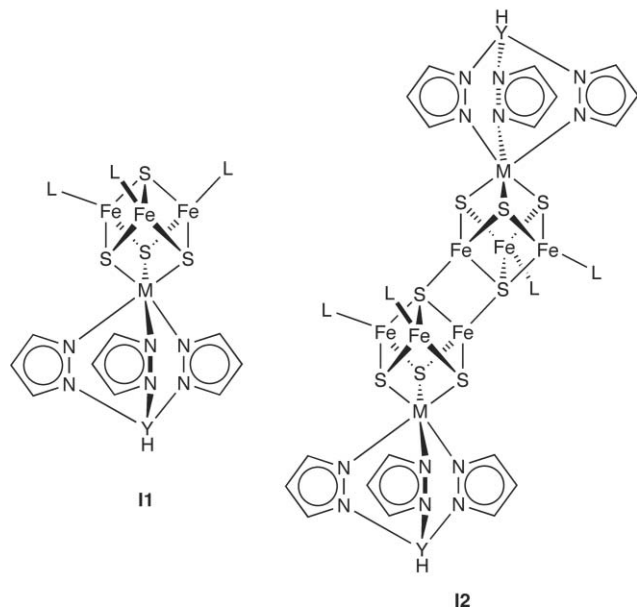
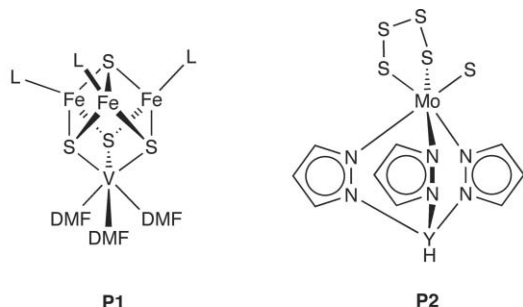


**M2** is the least satisfactory model, mainly because its lower connectivity allows excessive structural distortion. **M1** is the most promising, particularly when modified as in **M1A**, **M1B** to tie the back Fe atoms together and keep the front face open. Model **M1B** closely mimics FeMo-co in the calculations undertaken so far. **M1B** is also readily elaborated *via* the pyrazolyl-hydroborate or pyrazolyl-methane ligands to effect steric inactivation of the parts of the cluster that should not be reactive sites in an effective mimic. In addition, modification of the ligands in **M1B** to introduce a proton relay function should be relatively straightforward synthetically. Ligands very closely related to those in model **M1B-b** are known in the literature, *e.g.*<sup>84-86</sup> The carboxylate function in the ligands of the various **M1B** models, required to keep the *exo*-Fe<sub>A</sub>

and *exo*-Fe<sub>B</sub> coordination positions unconstrained, has precedent, and also could be replaced with alcoxide or thiolate functions, as for instance in the known ligands **LA**, **LB**.<sup>86</sup> There should be no difficulties in generating the functionalised tridentate ligands for the six-coordinate end M (Mo) atoms of proposed models.



The synthetic chemistry of cluster **M1** and its derivatives (including V in place of Mo) is well-developed. Note that the six-coordinate metal plays a largely structural role, and does not need to be Mo. The standard route starts with precursors **P1** or **P2**, both readily obtained,<sup>87</sup> and which allow the introduction of modified tridentate ligands at the six-coordinate metal. The first key intermediate is **I1**,<sup>87</sup> which, when L = PEt<sub>3</sub>, is converted to the edge-bridged double cubane structure **I2** by reduction with BH<sub>4</sub><sup>-</sup>.<sup>72,88</sup> A variety of reactions have been used to convert **I2** to **M1** derivatives,<sup>71,72,88</sup> including direct reaction of **I1** with **I2**.<sup>72</sup> Details of the ancillary ligands L and reaction conditions are given in the papers cited. The mechanism of the **I2** → **M1** conversion has been



studied.<sup>73</sup> The models **M1** are generally stable, but it is known that excess thiol or weak acid can cause reversion to **I2** or **I1**.<sup>72</sup>

There is no exact precedent for a synthetic reaction creating the proposed linkage of the rear Fe atoms of **M1**, as for instance in bridged **M1A**. Reactions substituting ligands L of **M1** are known,<sup>73</sup> and it could be that use of a bridging dithiolate ligand is feasible.

All of the models are electron-transfer active, as expected of metal-sulfide clusters, and therefore the introduction of electrons to the catalytic cycle, under homogeneous or heterogeneous (electrochemical) conditions, should be relatively straightforward. A key issue will be the matching of the operating redox potentials and the strength of the acid AH used to provide protons to the proton relay component, in order to introduce the H atoms onto the model cluster while avoiding the unwanted direct reduction of AH to H<sub>2</sub>. Redox potentials of specific models can be simulated prior to synthesis, using an existing correlation of redox potential and calculated HOMO energy.<sup>43</sup> Additional substituents on the ligands could be used to adjust potentials.

I note that the unmodified cluster systems **M1**, **M2**, **M3** and variants already reported were prepared under an atmosphere of N<sub>2</sub>, which was not bound. This is consistent with the proposed mechanism for FeMo-co, in which pre-hydrogenation of the cluster is required, to modify the coordination of Fe to enable N<sub>2</sub> binding. The enzyme needs to be reduced prior to N<sub>2</sub> binding.

Finally, I return to the metrical similarities between **M1** and the P<sup>N</sup> reduced-state P-cluster of nitrogenase, and speculate about functional similarities. Could the P-cluster in the MoFe protein of nitrogenase be a relic catalytic site for N<sub>2</sub> reduction, operating prior to the evolution of a more efficient FeMo-co site? A finding that **M1** (suitably protected and supported with electron- and proton-transfer functions) is able to catalyse the hydrogenation of N<sub>2</sub> would support this hypothesis.

## Progressing

I predict that **M1B-b**, or a model like it, is well-equipped to catalyse the hydrogenation of N<sub>2</sub> to NH<sub>3</sub>, given a suitable proton source AH and a suitable source of electrons (a homogeneous reductant or an electrochemical cell). The suggested first stage of investigation of this prediction is to secure the synthetic procedures, following the leading references cited above. Some exploration of synthetic methods to bridge or link the rear Fe atoms will be needed in this. As this progresses, guidance can come from further calculation of structure and stability of specific target molecules. Also needed in the synthetic effort will be investigation and adjustment of the redox potentials of models, and some exploration of possible proton shuttle functionalities, their base strengths, and compatible acids AH. A key milestone will be the isolation and characterisation of models with H atoms bound to S<sub>A</sub>, Fe<sub>A</sub> and/or Fe<sub>B</sub>. In conjunction with this, density functional simulation can examine the reactivities of species in hand, and provide energy profiles for possible catalytic steps.

The present article provides some direction for experimental investigation. Because density functional simulation can now explore, reliably and quickly, the structure and reactivity of mimicking clusters, progress will be advanced by collaborative theoretical and experimental investigation. As soon as some relevant clusters are in hand, the feasibility of them functioning as catalysts in mimicry of nitrogenase can be tested by calculation

of the reaction profiles for the proposed mechanism, as has been done for FeMo-co.

## Acknowledgements

This research is supported by the University of New South Wales and by the Australian National Computational Infrastructure.

## References

- 1 B. K. Burgess and D. J. Lowe, *Chem. Rev.*, 1996, **96**, 2983–3011.
- 2 J. Christiansen, D. R. Dean and L. C. Seefeldt, *Annu. Rev. Plant Physiol. Plant Mol. Biol.*, 2001, **52**, 269–295.
- 3 R. Y. Igarashi and L. C. Seefeldt, *Crit. Rev. Biochem. Mol. Biol.*, 2003, **38**, 351–384.
- 4 J. B. Howard and D. C. Rees, *Proc. Natl. Acad. Sci. U. S. A.*, 2006, **103**, 17088–17124.
- 5 L. C. Seefeldt, B. M. Hoffman and D. R. Dean, *Annu. Rev. Biochem.*, 2009, **78**, 701–722.
- 6 V. Smil, 'Enriching the Earth: Fritz Haber, Carl Bosch, and the Transformation of World Food Production', MIT Press, Cambridge, Massachusetts, 2001.
- 7 G. Ertl, *Angew. Chem., Int. Ed.*, 2008, **47**, 3524–3535.
- 8 J. Chatt, J. R. Dilworth and R. L. Richards, *Chem. Rev.*, 1978, **78**, 589–625.
- 9 R. A. Henderson, G. J. Leigh and C. J. Pickett, *Adv. Inorg. Chem.*, 1983, **27**, 197–292.
- 10 M. Hidai and Y. Mizobe, *Chem. Rev.*, 1995, **95**, 1115–1133.
- 11 M. Hidai, *Coord. Chem. Rev.*, 1999, **185–186**, 99–108.
- 12 G. J. Leigh, *J. Organomet. Chem.*, 2004, **689**, 3999–4005.
- 13 R. L. Richards, *Coord. Chem. Rev.*, 1996, **154**, 83–97.
- 14 D. Sellmann, *New J. Chem.*, 1997, **21**, 681–689.
- 15 M. D. Fryzuk and S. A. Johnson, *Coord. Chem. Rev.*, 2000, **200–202**, 379–409.
- 16 B. A. Mackay and M. D. Fryzuk, *Chem. Rev.*, 2004, **104**, 385–401.
- 17 M. D. Fryzuk, *Acc. Chem. Res.*, 2009, **42**, 127–133.
- 18 D. V. Yandulov and R. R. Schrock, *Science*, 2003, **301**, 76–78.
- 19 R. R. Schrock, *Acc. Chem. Res.*, 2005, **38**, 955–962.
- 20 J. D. Gilbertson, N. K. Szymczak and D. R. Tyler, *J. Am. Chem. Soc.*, 2005, **127**, 10184–10185.
- 21 J. D. Gilbertson, N. K. Szymczak, J. L. Crossland, W. K. Miller, D. K. Lyon, B. M. Foxman, J. Davis and D. R. Tyler, *Inorg. Chem.*, 2007, **46**, 1205–1214.
- 22 J. L. Crossland, L. N. Zakharov and D. R. Tyler, *Inorg. Chem.*, 2007, **46**, 10476–10478.
- 23 Y. Yu, A. R. Sadique, J. M. Smith, T. R. Dugan, R. E. Cowley, W. W. Brennessel, C. J. Flaschenriem, E. Bill, T. R. Cundari and P. L. Holland, *J. Am. Chem. Soc.*, 2008, **130**, 6624–6638.
- 24 L. D. Field, H. L. Li, S. J. Dalgarno and P. Turner, *Chem. Commun.*, 2008, 1680–1682.
- 25 L. D. Field, H. L. Li and A. M. Magill, *Inorg. Chem.*, 2009, **48**, 5–7.
- 26 J. L. Crossland, D. M. Young, L. N. Zakharov and D. R. Tyler, *Dalton Trans.*, 2009, 9253–9259.
- 27 R. H. Burris, *J. Biol. Chem.*, 1991, **266**, 9339–9342.
- 28 J. W. Peters, K. Fisher and D. R. Dean, *Annu. Rev. Microbiol.*, 1995, **49**, 335–366.
- 29 R. N. F. Thorneley and D. J. Lowe, *J. Biol. Inorg. Chem.*, 1996, **1**, 576–580.
- 30 J. B. Howard and D. C. Rees, *Chem. Rev.*, 1996, **96**, 2965–2982.
- 31 B. E. Smith, *Adv. Inorg. Chem.*, 1999, **47**, 159–218.
- 32 D. C. Rees and J. B. Howard, *Curr. Opin. Chem. Biol.*, 2000, **4**, 559–566.
- 33 D. C. Rees, F. A. Tezcan, C. A. Haynes, M. Y. Walton, S. Andrade, O. Einsle and J. A. Howard, *Philos. Trans. R. Soc. London, Ser. A*, 2005, **363**, 971–984.
- 34 J. H. Guth and R. H. Burris, *Biochemistry*, 1983, **22**, 5111–5122.
- 35 B. K. Burgess, S. Wherland, W. E. Newton and E. I. Stiefel, *Biochemistry*, 1981, **20**, 5140–5146.
- 36 J.-L. Li and R. H. Burris, *Biochemistry*, 1983, **22**, 4472–4480.
- 37 R. N. F. Thorneley and D. J. Lowe, in *Molybdenum enzymes*, ed. T. G. Spiro, Wiley Interscience, New York, 1985, p. 221–284.
- 38 O. Einsle, F. A. Tezcan, S. L. A. Andrade, B. Schmid, M. Yoshida, J. B. Howard and D. C. Rees, *Science*, 2002, **297**, 1696–1700.
- 39 I. Dance, *Chem. Commun.*, 2003, 324–325.
- 40 B. Hinnemann and J. K. Norskov, *J. Am. Chem. Soc.*, 2003, **125**, 1466–1467.
- 41 T. Lovell, T. Liu, D. A. Case and L. Noodleman, *J. Am. Chem. Soc.*, 2003, **125**, 8377–8383.
- 42 V. Vrajmasu, E. Munck and E. L. Bominaar, *Inorg. Chem.*, 2003, **42**, 5974–5988.
- 43 I. Dance, *Inorg. Chem.*, 2006, **45**, 5084–5091.
- 44 L. C. Seefeldt, I. G. Dance and D. R. Dean, *Biochemistry*, 2004, **43**, 1401–1409.
- 45 P. C. Dos Santos, S. M. Mayer, B. M. Barney, L. C. Seefeldt and D. R. Dean, *J. Inorg. Biochem.*, 2007, **101**, 1642–1648.
- 46 B. M. Barney, M. Laryukhin, R. Y. Igarashi, H.-I. Lee, P. C. Dos Santos, T.-C. Yang, B. M. Hoffman, D. R. Dean and L. C. Seefeldt, *Biochemistry*, 2005, **44**, 8030–8037.
- 47 R. Y. Igarashi, M. Laryukhin, P. C. Dos Santos, H.-I. Lee, D. R. Dean, L. C. Seefeldt and B. M. Hoffman, *J. Am. Chem. Soc.*, 2005, **127**, 6231–6241.
- 48 B. M. Barney, H.-I. Lee, P. C. Dos Santos, B. M. Hoffman, D. R. Dean and L. C. Seefeldt, *Dalton Trans.*, 2006, 2277–2284.
- 49 B. M. Barney, J. McClead, D. Lukoyanov, M. Laryukhin, T. C. Yang, D. R. Dean, B. M. Hoffman and L. C. Seefeldt, *Biochemistry*, 2007, **46**, 6784–6794.
- 50 B. M. Hoffman, D. R. Dean and L. C. Seefeldt, *Acc. Chem. Res.*, 2009, **42**, 609–619.
- 51 B. M. Barney, D. Lukoyanov, R. Y. Igarashi, M. Laryukhin, T.-C. Yang, D. R. Dean, B. M. Hoffman and L. C. Seefeldt, *Biochemistry*, 2009, **48**, 9094–9102.
- 52 S. C. Lee and R. H. Holm, *Proc. Natl. Acad. Sci. U. S. A.*, 2003, **100**, 3595–3600.
- 53 S. C. Lee and R. H. Holm, *Chem. Rev.*, 2004, **104**, 1135–1157.
- 54 S. Groysman and R. H. Holm, *Biochemistry*, 2009, **48**, 2310–2320.
- 55 T. H. Rod, B. Hammer and J. K. Norskov, *Phys. Rev. Lett.*, 1999, **82**, 4054–4057.
- 56 F. Barriere, M. C. Durrant and C. J. Pickett, in *Catalysts for Nitrogen Fixation. Nitrogenases, Relevant Chemical Models and Commercial Processes*, ed. B. E. Smith, R. L. Richards and C. J. Pickett, Kluwer Academic Publishers, Netherlands, 2004, p. 161–199.
- 57 L. Noodleman, T. Lovell, W.-G. Han, J. Li and F. Himo, *Chem. Rev.*, 2004, **104**, 459–508.
- 58 Z. X. Cao, X. Jin and Q. N. Zhang, *J. Theor. Comput. Chem.*, 2005, **4**, 593–602.
- 59 Z. Cao, X. Jin, Z. Zhou and Q. Zhang, *Int. J. Quantum Chem.*, 2006, **106**, 2161–2168.
- 60 J. Kastner and P. E. Blochl, *ChemPhysChem*, 2005, **6**, 1724–4.
- 61 J. Kastner, S. Hemmen and P. E. Blochl, *J. Chem. Phys.*, 2005, **123**, 074306.
- 62 J. Kastner and P. E. Blochl, *J. Am. Chem. Soc.*, 2007, **129**, 2998–3006.
- 63 L. Noodleman and W.-G. Han, *J. Biol. Inorg. Chem.*, 2006, **11**, 674–694.
- 64 V. Pelmenschikov, D. A. Case and L. Noodleman, *Inorg. Chem.*, 2008, **47**, 6162–6172.
- 65 I. Dance, *Chem.–Asian J.*, 2007, **2**, 936–946.
- 66 I. Dance, *J. Am. Chem. Soc.*, 2005, **127**, 10925–10942.
- 67 I. Dance, *J. Am. Chem. Soc.*, 2007, **129**, 1076–1088.
- 68 I. Dance, *Biochemistry*, 2006, **45**, 6328–6340.
- 69 I. Dance, *Dalton Trans.*, 2008, 5977–5991.
- 70 I. Dance, *Dalton Trans.*, 2008, 5992–5998.
- 71 Y. Zhang and R. H. Holm, *Inorg. Chem.*, 2004, **43**, 674–682.
- 72 Y. Zhang and R. H. Holm, *J. Am. Chem. Soc.*, 2003, **125**, 3910–3920.
- 73 C. P. Berlinguette and R. H. Holm, *J. Am. Chem. Soc.*, 2006, **128**, 11993–12000.
- 74 C. P. Berlinguette, T. Miyaji, Y. Zhang and R. H. Holm, *Inorg. Chem.*, 2006, **45**, 1997–2007.
- 75 M. L. Hlavinka, T. Miyaji, R. J. Staples and R. H. Holm, *Inorg. Chem.*, 2007, **46**, 9192–9200.
- 76 J.-L. Zuo, H.-C. Zhou and R. H. Holm, *Inorg. Chem.*, 2003, **42**, 4624–4631.
- 77 H.-C. Zhou, W. Su, C. Achim, P. V. Rao and R. H. Holm, *Inorg. Chem.*, 2002, **41**, 3191–3201.
- 78 G. Henkel, H. Strasdeit and B. Krebs, *Angew. Chem., Int. Ed. Engl.*, 1982, **21**, 201–202.
- 79 H. Strasdeit, B. Krebs and G. Henkel, *Inorg. Chem.*, 1984, **23**, 1816–1825.
- 80 K. S. Hagen, A. D. Watson and R. H. Holm, *J. Am. Chem. Soc.*, 1983, **105**, 3905–3913.

- 
- 81 F. Osterloh, W. Saak, S. Pohl, M. Kroeckel, C. Meier and A. X. Trautwein, *Inorg. Chem.*, 1998, **37**, 3581–3587.
- 82 T. Lovell, J. Li, T. Liu, D. A. Case and L. Noodleman, *J. Am. Chem. Soc.*, 2001, **123**, 12392–12410.
- 83 J. Schimpl, H. M. Petrilli and P. E. Blochl, *J. Am. Chem. Soc.*, 2003, **125**, 15772–15778.
- 84 A. Beck, B. Welbert and N. Burzlaff, *Eur. J. Inorg. Chem.*, 2001, 521–527.
- 85 B. Kozlevcar, P. Gamez, R. de Gelder, W. L. Driessen and J. Reedijk, *Eur. J. Inorg. Chem.*, 2003, 47–50.
- 86 J. N. Smith, J. T. Hoffman, Z. Shirin and C. J. Carrano, *Inorg. Chem.*, 2005, **44**, 2012–2017.
- 87 D. V. Fomitchev, C. C. McLauchlan and R. H. Holm, *Inorg. Chem.*, 2002, **41**, 958–966.
- 88 Y. Zhang, J.-L. Zuo, H.-C. Zhou and R. H. Holm, *J. Am. Chem. Soc.*, 2002, **124**, 14292–14293.